

## COMPUTATIONALLY EFFICIENT, YET ROBUST, COASTAL FLOOD RISK ANALYSIS USING A REDUCED COMPLEXITY INUNDATION MODEL AND METAMODEL

A. Rueda<sup>1</sup>, B. Gouldby<sup>2</sup>, F.J. Méndez<sup>1</sup>, A. Tomás<sup>1</sup>, I.J., Losada<sup>1</sup>, J.L. Lara<sup>1</sup> and P. Díaz-Simal<sup>1</sup>

1. Environmental Hydraulics Institute "IH Cantabria", Universidad de Cantabria, Spain

2. HR Wallingford, UK

**ABSTRACT:** To effectively manage coastal flood risk it is necessary to be able to quantify it. This quantification can however, be a challenging undertaking. Coastal flooding risk is defined as the probability of flooding multiplied by the consequences. However, both the probability of flooding and the consequences can vary significantly over broad spatial and temporal scales. The probability component of coastal flood risk it is usually calculated by the application of multivariate extreme value models that extrapolate the joint probability density of the historical data, normally defined by the offshore sea condition (wave height, wave period, wave direction, wind intensity and direction, astronomical tide, storm surge level, mean sea level), to extreme values. Executing the corresponding hydrodynamic and inundation models for the full set of stochastically generated events is often not viable in computational terms. In the study described here, a computationally efficient, and hence practical, coastal flood risk analysis modelling system has been developed. The system applies the multivariate extreme value model of Heffernan and Tawn (2004) to high resolution offshore sea condition data (Camus et al, 2013). The resulting monte-carlo simulation data are then transferred inshore using a meta-modelling approach based on data mining techniques and non-linear interpolation functions (Camus et al 2011). These transformed nearshore data then form the boundary conditions of a reduced complexity (and hence computationally efficient) flood inundation model (RFSM-EDA). The modelling system has been applied to an urban coastal area located at Northern Spain mainly affected by wave-induced overtopping events.

Key Words: Coastal flood risk, Data mining, Multivariate extreme value methods, Surge, Wind-waves

### 1. INTRODUCTION

Coastal flood risk may be quantified by the probabilities of flood events and their potential consequences (Samuels *et al.*, 2005) and is usually expressed in monetary terms (e.g. €/year). Historical records of extreme values of the ocean variables responsible of flooding are limited therefore some statistical methods have been developed to infer the probability distribution of inundation events from the storm statistics, such as the Joint Probability Method (JPM). These inundation events (offshore sea conditions) must be transferred to consequences following the commonly adopted source-pathway-receptor-consequences model. The main objective of this article is to develop a new methodology to assess the full distribution of flood risk using a highly efficient 2D flood model and applying empirically-based depth-damage functions to estimate the statistical distribution and spatial extent of damage.

### 2. METHODOLOGY

In common with other natural hazard analysis, flood risk ( $R$ ) is typically defined as a function of probability and consequence ( $Z$ ) and expressed in terms of Expected Annual Damage (EAD), USACE (1996). In the context here, the probability component comprises consideration of multiple sea condition variables and hence can be written as:

$$R = E[Z] = \int_0^{\infty} f_X(X) g(X) dx \quad [1]$$

where  $X$  is a vector comprising the sea condition variables and  $f_X(X)$  is the joint probability density of the sea-conditions. The consequences of flooding are a function,  $g$ , of the sea conditions. The natural starting point for the analysis is offshore sea conditions in deep water away from the nearshore region where waves undergo complex transformation processes, (Bruun and Tawn, 1998). The joint probability density of offshore sea conditions is extrapolated to extreme values using the method of Heffernan and Tawn (2004). This analysis provides a stochastically generated set of peak values of sea-conditions, which includes extremes and preserves the dependence characteristics of the original data. This set of events is transformed to nearshore using a meta-model constructed using the SWAN (Booij et al., 1999) wave transformation model. These nearshore peak sea-condition events are then used to calculate overtopping rates based on a pre-run library of IH2VOF (Torres-Freyermouth et al., 2007) cases under different profile typologies. The corresponding overtopping rates form the boundary conditions for flood inundation simulations, which are undertaken with a computationally efficient flood inundation model, RFSM EDA, (Jamieson *et al.*, 2012a). The resulting outputs are aggregated to determine risk. The different steps of the modelling system are summarized in Figure 1 and described in detail throughout the specific case study.

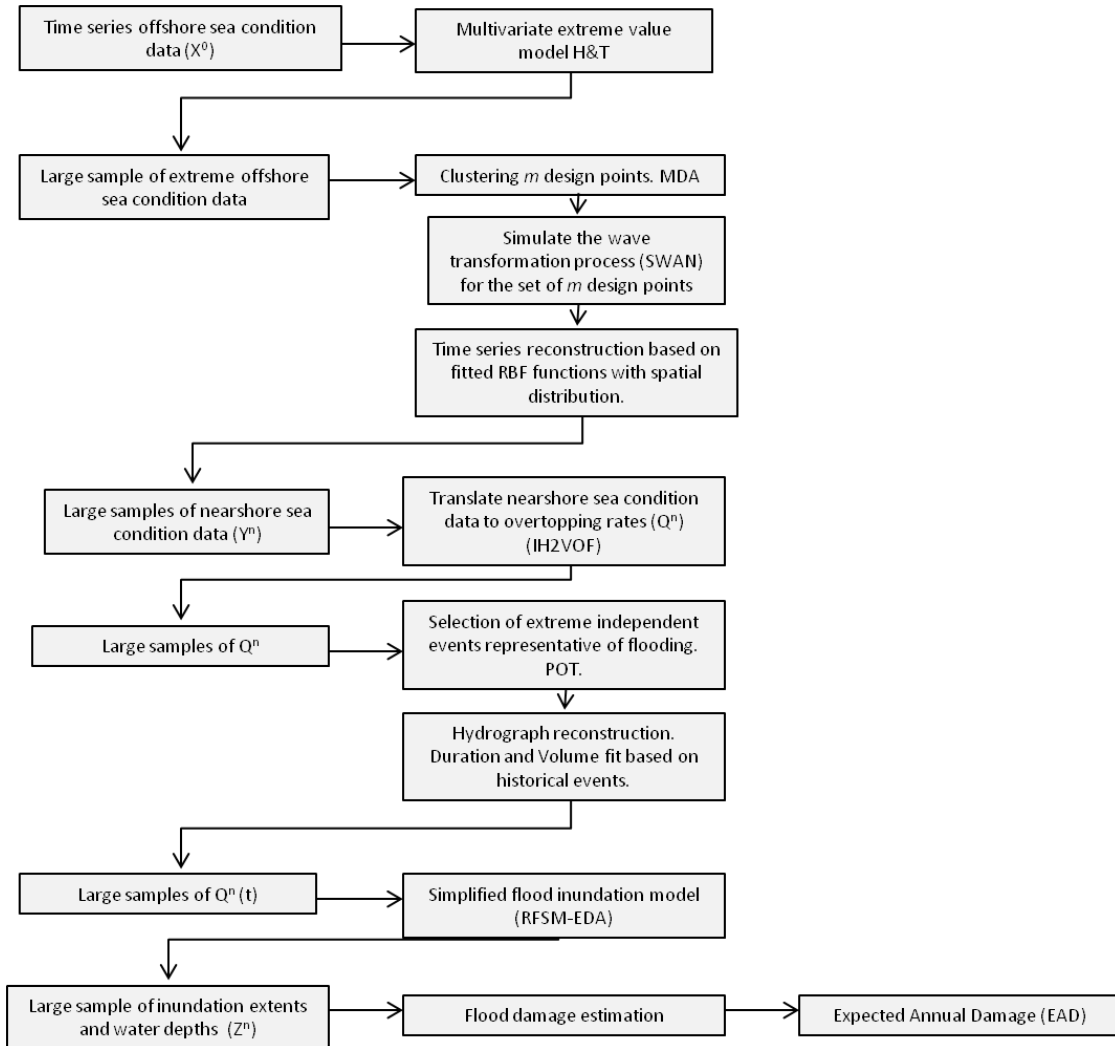


Figure 1: Methodology Flow Chart

### 3. CASE STUDY

The location chosen for the case study site is Sardinero Beach at the coastal town of Santander on the Cantabria Coast in northern Spain. This coastal area is sporadically affected by large swells generated in the North Atlantic basin (significant wave height up to 10m, storm surge level up to 2m and spring tide up to 5m) producing important wave-induced overtopping events. Sardinero is an urban sandy beach very popular due to the recreation amenities throughout the year for both residential and tourism purposes. The beach and the city are separated by a promenade at different heights along it (Figure 2). The studied urban area is mostly residential with spacious recreational zones. It is one of the most noted parts of the city.

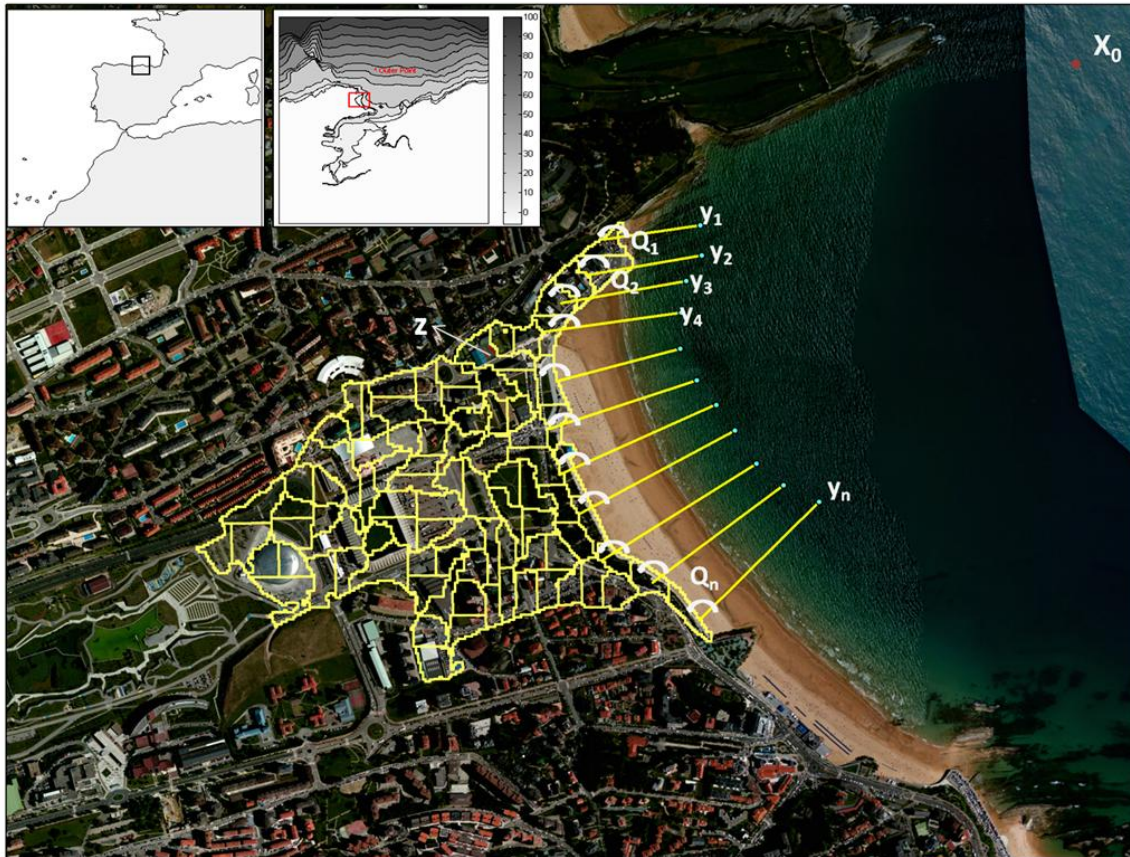


Figure 2: Map of the study location, nearshore points (clear blue), IH2VOF profiles and RFSM-EDA computational mesh (yellow).

#### 3.1 Data

The global wave hindcast GOW, (Reguero *et al.*, 2012), has been used as the primary source of wave data for this study. This reanalysis data set uses the Wave Watch III numerical model forced by 6-hourly wind fields from the atmosphere model NCEP/NCAR. The reanalysis GOW spans from 1948-2013 with hourly resolution. These data have been further downscaled to regional scale to obtain a Downscaled Ocean Waves (DOW) database, (Camus *et al.*, 2013). The DOW data comprise hourly data for the period 1948-2013 with spatial resolution of  $\sim 200$  m along the Spanish coast. These data have been calibrated using instrumental records (Mínguez *et al.*, 2011).

Sea level data (astronomical and surge residuals) in the form of hourly time series from two different tide gauges, the Spanish Institution of Oceanography (1940-2005) (IEO) and from Puertos del Estado (1995-

present), were used in the analysis. Where there were gaps in the time series, these were filled using a regional storm surge reanalysis of southern Europe, GOS (Cid *et al.*, 2013).

The topographic data is obtained from a national topographic map 1:25000 (MTN25) from the National Geographic Institute, resampled to a 5 meters horizontal resolution DTM. The bathymetry used is defined by means of the global bathymetry “General Bathymetric Chart of the Oceans” (GEBCO), with a spatial resolution of 1’ from a combination of sounding waves and satellite data, available at the British Oceanographic Data Centre (BDOC), and the Spanish coastal charts, providing a detailed representation of the shallow water areas.

### 3.2 Multivariate Extreme Value Method

A joint probability method, that has as its basis the approach of Heffernand and Tawn (2004), is adopted to obtain the large sample of offshore multivariate extreme dataset necessary to characterize risk. The methodology is described in detail in Gouldby *et al.* (2014) and is summarized briefly here.

The offshore variables considered on the case study site comprised waves (height ( $H_s$ ), mean period ( $T_m$ ) and direction ( $\theta_{Hs}$ )), winds (speed ( $U$ ) and direction ( $\theta_U$ )), sea level (surge ( $S$ ) and astronomical component ( $A$ )) that can combine to induce flooding.

The problem then is to determine the probability of exceeding specified levels of a flood consequence related variable of interest. This could be the number of injuries or fatalities, for example, or alternatively economic damage. Often intermediate variables such as depth or velocity of flooding are required for mapping purposes. In this case study water depth in the floodplain is the variable of interest and is denoted as  $Z$ , hence the requirement is to establish:

$$\Pr(Z > z) = \Pr(g(\mathbf{X}^o) > z) \quad [2]$$

Whilst there are alternatives, there are significant benefits in employing joint probability methods (JPM), (Bruun and Tawn (1998), Hawkes *et al.* (2002) and Gouldby *et al.* (2014)). These JPM methods require extrapolation of the joint density of  $\mathbf{X}^o$  to extremes and then integration over the region  $\Delta(\mathbf{X}^o) > z$ :

$$\Pr(Z > z) = \int_{Z > z} f_{\mathbf{X}^o}(\mathbf{X}^o) d\mathbf{X}^o \quad [3]$$

The JPM approach is adopted here and the extrapolation of the joint probability density is undertaken using the method of Heffernan and Tawn (2004). This evolves by first specifying semi-parametric marginal distributions, with the extremes defined by Generalised Pareto Distributions (GPD’s) which are transformed onto Gumbel scales. If  $Y_{-i}$  denotes the vector of all transformed variables  $Y_j$  excluding  $Y_i$ , the method is typically applied using the multivariate non-linear regression model

$$Y_{-i} | Y_i = a Y_i + Y_i^b W \quad \text{for } Y_i > v, \quad [4]$$

where  $a$  and  $b$  are vectors of the parameters from the fitted pair-wise regression model,  $v$  is a specified threshold and  $W$  is a vector of the regression residuals. The residuals are assumed to be normally distributed with a mean and standard deviation to be found and maximum likelihood is generally used to obtain the parameter estimates. Once fitted, a Monte Carlo simulation procedure is used whereby samples from the residuals are used to generate realisations of  $Y$ . These are then transformed back to the original scales. The result is a large (in this case approximately 314,000 realisations, representative of 10,000 years) set of offshore sea condition events.

### 3.3 Nearshore Data

To proceed with the analysis, it is necessary to transform the stochastically generated set of offshore conditions through to the nearshore. Transformation of the large set of offshore sea conditions may often not be practical due to computational resource constraints. To overcome this constraint, a meta-model of SWAN has been developed. Whilst there are a wide variety of meta-modelling methods, Camus *et al.* (2011), has used Radial Basis Functions (RBF's) to replicate the SWAN wave model and hence that approach is chosen here. The RBF has the following form:

$$Y^N = p(\mathbf{X}^o) + \sum_{i=1}^m a_i \Phi(\|\mathbf{X}^o - \mathbf{D}\|) \quad [5]$$

Here,  $Y^N$  is the vector of the near-shore sea conditions (ie the output of the meta-model) and:

$$p(\mathbf{X}^o) = b_0 + b_1 X_1^o + b_2 X_2^o \dots + b_n X_n^o \quad [6]$$

$b_{0,1,2..n}$  are coefficients to be found by fitting the RBF to the known points and  $\Phi$  is a Gaussian function defined as:

$$\Phi(\|\mathbf{X}^o - \mathbf{D}\|) = \exp\left(-\frac{\|\mathbf{X}^o - \mathbf{D}\|^2}{2c^2}\right) \quad [7]$$

where  $c$  is a shape parameter  $D$  is a vector comprising the  $m$  "known" near-shore wave conditions derived from the SWAN model design point simulations.

Once fitted, the RBF's are used in place of the SWAN model to transfer the offshore data a series of nearshore locations (Figure 2). The number of design points ( $m$ ) used to construct the meta-model was  $m=500$ . The MDA was run to define these design points. These points are shown, together with the simulated and historical data, in Figure 3.

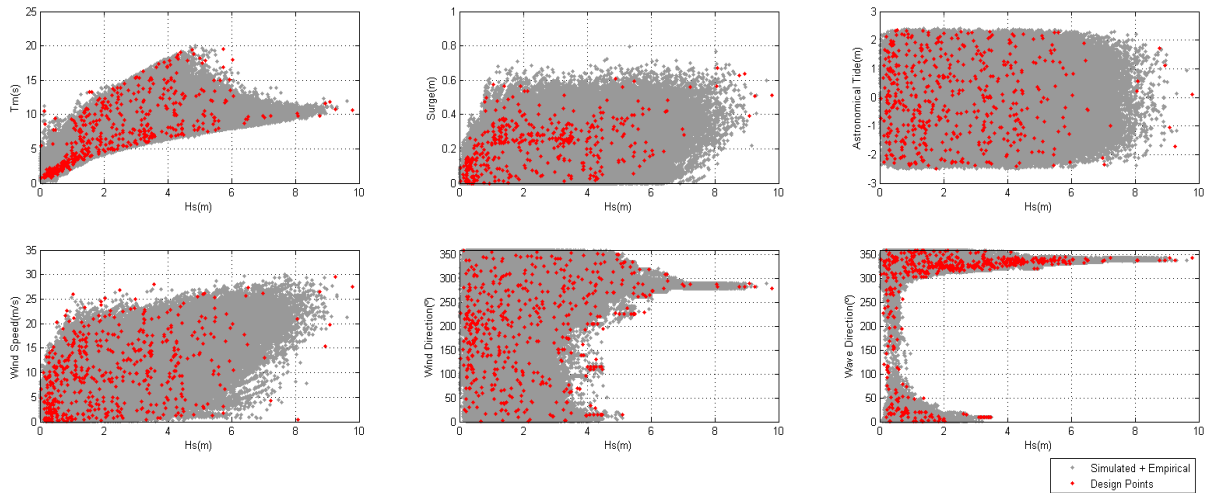


Figure 3: Simulated offshore data and design points output from the MDA algorithm.

### 3.4 Overtopping Rates

Overtopping rates were numerically modeled with IH2VOF model ([www.ih2vof.ihcantabria.com](http://www.ih2vof.ihcantabria.com)). IH2VOF is one of the most advanced RANS models due to its capabilities, robustness and extensive validation for both surf zone hydrodynamics (Torres-Freyermuth et al., 2007) and the stability and functionality of conventional or non-conventional coastal structures. This model solves the two-dimensional wave-flow for hybrid domains in a coupled NS-type equation system, at the clear-fluid region (outside the porous media) and inside the porous media by the resolution of the Volume-Averaged Reynolds Averaged Navier-Stokes (VARANS) equations. Turbulence is modelled using a  $k-\epsilon$  model for both the clear-fluid region and the porous media region. Realistic wave generation, second order generation and active wave absorption are some of the unique features included in the model.

As a RANS-VOF model is highly computationally expensive, data-mining techniques (Camus et al. 2011), were used to define a subset of sea states that were then used as input to RANS-VOF model. The output results were used to define a catalogue of results that were used within the stochastic analysis. The selection was made taking into consideration the sea level (astronomical tide and storm surge) and the wave parameter  $(H_0 L_0)^{0.5}$  ( $H_0$  is the significant wave height and  $L_0$  is the peak period deep-water wave length).

Figure 4 shows the historical time series reconstruction of the offshore point ( $X_0$ ), a local point ( $Y_6$ ) and the associated hourly averaged overtopping rates ( $Q_6$ ) in section number "6".

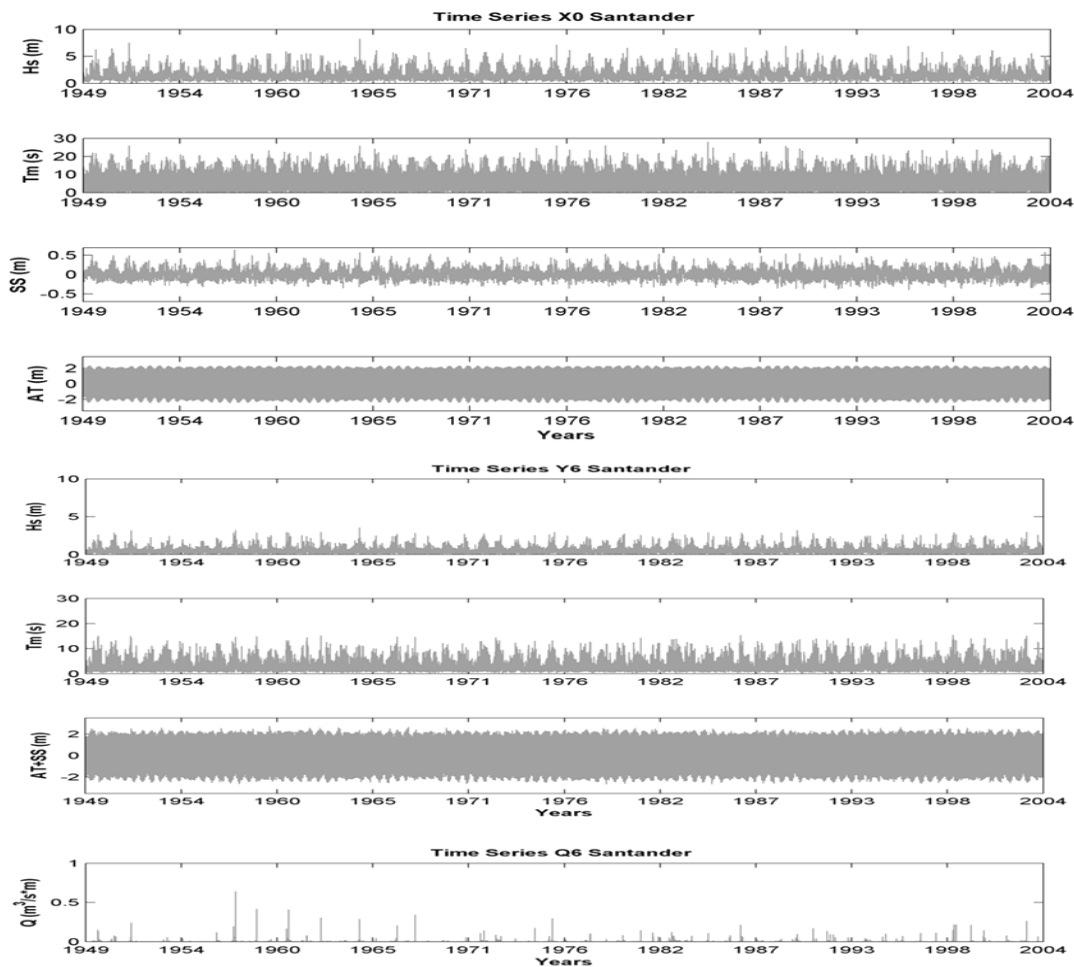


Figure 4: Historical Time Series Reconstruction from offshore data to overtopping rates (top to bottom).

To proceed with the analysis it is necessary to define the hydraulic boundary conditions input to the inundation model, namely the associated hydrograph  $Q^n(t)$  for each of the stochastically simulated peak events. For practical purposes, the design hydrographs have been kept simple while synthesizing and preserving some physical properties (such as peak discharge  $Q$ , volume  $V$ , duration  $D$ , and hydrograph shape) (Serinaldi, et al., 2011). In this study, a triangular hydrograph shape has been assumed dependent on these three parameters  $s$ . The physical properties of each simulated hydrograph are based on historical information where the events chosen are those with an overtopping rate representative of flooding ( $>0.1\text{m}^3/\text{s}$ ). The historical data used is selected with the standard peaks-over-threshold approach and the corresponding duration, and total volume of each event has been calculated.

With these examples of observed hydrographs a relationship has been established between peak overtopping rate and its corresponding duration (Figure 5). Using this relationship a synthetic hydrograph for each stochastically simulated sea-state, can be defined and used as input for the inundation model.

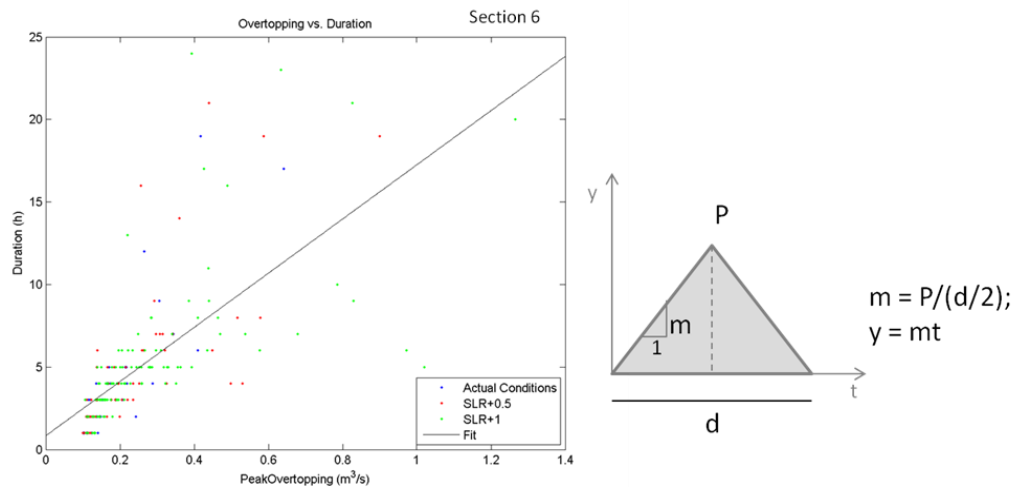


Figure 5: Example of a Duration Fit (section 6) (left) and Synthetic Hydrograph scheme (right).

### 3.5 Flooding Model

There are a wide variety of numerical models available for simulating flood events. These range in complexity from simplified sea level projection methods, to volume spreading methods (Gouldby *et al.*, 2008a) diffusion wave methods (Bates and De Roo, 2000) and models that solve the full shallow water equations (Lhomme *et al.* 2010), for example. The simplified models have been widely applied in probabilistic analyses due to their computational efficiency. This efficiency is however, often obtained at the expense of accuracy of the predicted flooding scenario. More recently, new hybrid diffusion wave/full SWE models have emerged, (Bates *et al.*, 2010). In this approach, a local acceleration term is included with only the advection term of the full shallow water equations excluded. This additional term enables stable solutions at much larger time steps, thereby significantly increasing computational efficiency when compared to standard diffusion wave models. High resolution (1-2m horizontal) LIDAR data is increasingly being used for flood inundation simulations. Running numerical models at this resolution can, depending on the size of the study area and model formulation, be exceptionally computationally demanding. To make use of this detailed information, whilst still achieving practical simulation times, a new model has been developed. This model, RFSM EDA, (Jamieson *et al.*, 2012a) stems from earlier modelling systems used for national and regional flood risk analysis in England and Wales, (Gouldby *et al.* 2008a).

The RFSM-EDA model operates on a topographically based mesh enabling model simulations to be undertaken at coarse resolution, offering significant increases in computational efficiency when compared with traditional (flat cell) models (Jamieson *et al.*, 2012). This meshing system requires the analysis of the

floodplain topography using a pre-processing algorithm to develop an irregular mesh of so-called Impact Zones (Figure 2). The resolution of the Impact Zones mesh is not dependant on the DTM resolution as the user can control the minimum and maximum size of the Impact Zones. Therefore a fine resolution DTM can be used to produce the mesh of Impact Zones with no impact on the number of Impact Zones (and the model runtime). The flow calculations that are performed on the coarse mesh are defined using the set of equations proposed by Bates et al. (2010). This offers further computational efficiencies over diffusion wave models that use the same meshing system, (Falter *et al.*, 2012), due to the increased time steps that are possible.

The topographically based nature of the mesh requires a slightly different approach than that applied by Bates et al. (2010). The flow across each cell interface,  $Q_f$ , is given by

$$Q_f^{t+\Delta t} = \frac{(Q_f^t - g\Delta t A_f^t S_f^t)}{1 + g\Delta t n^2 |Q_f^t| / A_f^t (R_f^t)^{4/3}} \quad [8]$$

Where  $Q_f$  is the interface flow,  $t$  is time,  $A_f$  is interface area,  $R_f$  is hydraulic radius of the interface,  $n$  is Manning's coefficient and  $S_f$  is the water surface slope across the interface. Conservation of mass is ensured through the implementation of Eqn. 9.

$$V_i^{t+\Delta t} = V_i^t + \Delta t \sum_j Q_f^{t+\Delta t} \quad [9]$$

where  $V_i$  is the volume in Impact Zone  $i$ , and  $j$  is a neighboring cell. The volume within each Impact Zone ( $V_i$ ) is a function of the water level. These relationships are defined in advance during a pre-processing stage, enabling efficient computation during the simulation. The equations are solved using an adaptive time-step. Numerical stability is ensured through implementation of a CFL criterion developed by Guinot and Soares-Frazão (2006). Overall the RFSM EDA results have proved to be closely comparable to those from full SWE models (Environment Agency 2013, Jamieson *et al.*, 2012).

Due to the fast simulation run times, less than 10 seconds on a standard desktop computer for the study area, it is possible to simulate a large number of events, those from the simulated dataset that are representative of flooding (overtopping rate higher than 0.1 m<sup>3</sup>/s in any of the defined sections). The number of RFSM-EDA realizations are 69926. Figure 6 shows an example of the simulations performed associated with an extreme event that recently occurred. On the right hand side, a picture taken on March, 1st, 2014 reveals a dramatic storm event that recently affected the study area.



Figure 6 : (Left) Inundation extent and reached water depth (test 20587).(Right) Picture taken on March 1st, 2014 during an exceptional event.



### 3.6 Damage Model

The last step is to calculate the flood damage for every scenario simulated. Although, in the literature a broad set of flood functions can be found, some general properties can describe the differences: (1) functions may express damage as marginal function or as integral function: in the first case additional damage is calculated for each increase in depth and in the second as total damage due to each water level. The different approaches have different purposes, the first one is used to determine the optimum level of any flood protection measure, and the second is used to determine total damage from each hazard level; (2) Thresholds: Damages may exist only when the hazard overpasses a certain threshold. If this is the case, there is a minimum value for hazard required for damage to exist; (3) Convexity/Concavity: If for all depths  $h > k$ ,  $\frac{\partial D}{\partial h} > 0$ ;  $\frac{\partial^2 D}{\partial h^2} < 0$  meaning that total damage is increasing but at a decreasing rate there is convexity. However, concavity exists at a level that once has been reached produces the maximum damage (collapse of the system) and no additional increase in hazard level would produce additional damage.; (4) Local versus global effects. There may be damages directly related to the flood location or conversely the impact of the flooding may reach areas distant from the flooded area through the services produced in a social or economic network. In our case, we have identified an electrical facility (land use 9) that provides services to a broad area that may suffer indirect damages if the facility is disconnected from the network. This fact exemplifies the issue that direct damages are directly observed in the field but indirect damages may travel to non flooded areas.

To be able to calculate the expected damage the asset value and the damage functions have to be assigned to the different land-use units. Different databases can be consulted such as the Multi Coloured Manual (UK) (Penning-Rowsell et al. 2003), HAZUSMH multi-hazard software (United States)(Fema,2009) or the JRC Model (European Commission/HKV)(Huizinga, 2007) where more general damage functions are defined, however in this study we have opted for a specific definition of the damage functions based on local data and expert judgment, which is recommended for micro-studies to reduce uncertainties (Buck 2004). In the case study nine different land uses have been defined (figure 7). Based on the properties from table of figure 7, a Beta CDF-type damage curve has been assigned to each land use. Therefore, the estimated damage can be described as follow:

$$\text{Damage}_{\text{unit } i} = \text{AssetValue}_i * \text{CDF}((x - x_{\text{mini}})/(x_{\text{maxi}} - x_{\text{mini}})) \quad [10]$$

where the cumulative distribution function CDF is defined by a Beta distribution family of Beta(2,2),  $x_{\text{min}}$  is the threshold where damage starts and  $x_{\text{max}}$ , the water depth at which damage stops to increase.



Code	Description	Uses	Thresholds (cm)	Maximum depth (cm)	Damage waves/depth	Indirect Damage	Asset Value (€km <sup>2</sup> )
001	Urban Park-Garden	Recreational	5	150	(W) (D)	No	20
002	Business/Commercial	Economic/Consumer Supply	20	100	(D)	Yes	150
003	Urbanized pedestrian walk	Recreational	30	150	(W)	No	60
004	Residential areas	Residence	10	100	(D)/(W)	Yes	180
005	Residential areas	Parking	10	50	D	Yes	70
006	Hotels	Touristic	20	100	D	Yes	150
007	Parking	Services	30	180	D	Yes	20
008	Sporting activities	Services	5	50	D	Yes	110
009	Electric Infrastructure	Infrastructure	20	100	(D)	Yes	20,000

Figure 7: Land Uses Units.

To calculate the total damage of each stochastic realisation the damage of each cell within the flood plain must be summed up.

The last step to calculate flood risk or the expected annual damage (EAD) is the integration of the total risk over the 10000 simulated years.  $EAD = \sum D_k / \text{years}$ ; where  $k$  account for each of the simulated events. In our example, the EAD for Sardinero beach is 0.8M€. With the large set of simulated events it is possible to obtain different statistical outputs such as the inundation map and spatial expected damage for a certain return period. As an example in figure 8, the 100 year return period event related to the water depth in the floodplain and its corresponding damage are presented.

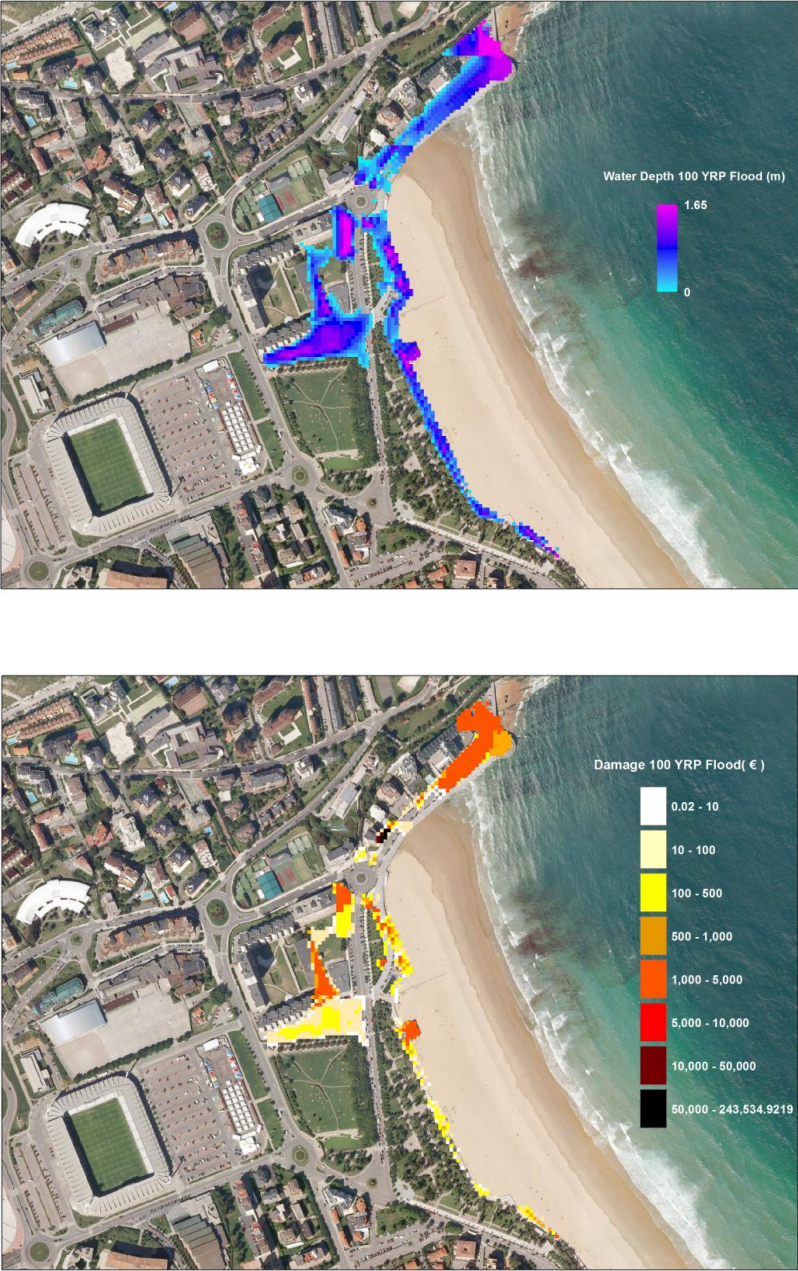


Figure 8: 100 year return period flood depth in the floodplain (top) and its associated damage (bottom). Spatial units are  $5 \times 5 = 25 \text{m}^2$ .

#### 4. CONCLUSIONS

A computationally efficient, yet robust coastal flooding risk model has been described. For simplicity, the methodology has been applied to a small urban area in northern Spain, but one of its advantages is that it could be extended to larger spatial scales since the extreme value method is applied in deep water and the processes that the waves experience in their travel to coast such as shoaling, refraction..etc are modeled with hydrodynamic and surf zone models in a computationally efficient manner with the use of metamodels and a pre-executed library respectively. The use of a validated simplified inundation model to compute the inundation extents and water depth allows to simulate the large sample of extreme independent cases preserving the key hydraulic principles of mass conservation and flow connectivity, allowing the determination of the statistical distribution of damage and its spatial distribution.

Future work in this area is needed to incorporate different aspects such as an efficient defence reliability analysis, which would improve the current methodology, and the identification and quantification of the uncertainties associated with every particular component.

#### 5. REFERENCES

- Bates, P. D. and De Roo, A. P. J. 2000: "A simple raster-based model for flood inundation simulation." *Journal of Hydrology* 236: 54-77.
- Bates, P. D., Horritt, M. S. and Fewtrell, T. J. 2010: "A simple inertial formulation of the shallow water equations for efficient two-dimensional flood inundation modelling." *Journal of Hydrology* 387(12): 33-4
- Booij, N., Ris, R. C. and Holthuijsen, L. H. 1999: "A third-generation wave model for coastal regions: 1. Model description and validation." *Journal of Geophysical Research: Oceans* 104(C4): 7649-7666.
- Bruun, J. T. and Tawn, J. A. 1998: "Comparison of approaches for estimating the probability of coastal flooding." *Journal of the Royal Statistical Society: Series C (Applied Statistics)* 47(3): 405-423.
- Buck W. 2004. *Monetary evaluation of flood damages*, In: D. Mahlzahn, T. Plapp. (Eds.): *Disasters and Society , From Hazard Assessment to Risk Reduction*, Int. Conf. July 2004, Karlsruhe, Berlin: Logos Verl. 2004, p. 123 - 127
- Camus, P., Mendez, F. J. and Medina, R. 2011: "A hybrid efficient method to downscale wave climate to coastal areas." *Coastal Engineering* 58(9): 851-862.
- Camus, P., Mendez, F.J., Medina, R., Tomás, A., Izaguirre, C. 2013: "High resolution downscaled ocean waves (DOW) reanalysis in coastal areas", *Coastal Engineering*, 72, 56-68.
- Cid, A., Castanedo, S., Abascal, A. J., Menéndez, M., Medina, R. 2014. "A high resolution hindcast of the meteorological sea level component for Southern Europe: the GOS dataset". *Climate Dynamics*. doi:10.1007/s00382-013-2041-0
- Davison, A. C. and Smith, R. L. 1990. "Models for exceedances over high thresholds." *Journal of the Royal Statistical Society, Series B (Statistical Methodology)* 52(3): 393-442.
- Environment Agency 2010 "Benchmarking of 2D Hydraulic Modelling Packages", *Environment Agency Report SC080035/SR2*, Bristol
- Gouldby, B., Sayers, P., Mulet-Marti, J., Hassan, M. and Benwell, D. 2008a. "A methodology for regional-scale flood risk assessment." *Water Management* 161(3): 169-182.
- Gouldby, B., Sayers, P. and Tarrant, O. 2008b. "Application of a flood risk model to the Thames Estuary for economic benefit assessment". *Risk Analysis VI :Simulation and Hazard Mitigation, Caephalonia, WITpress*.
- Guinot, V. and Soares-Frazão, S. (2006). "Flux and source term discretization in two-dimensional shallow water models with porosity on unstructured grids." *International Journal for Numerical Methods in Fluids* 50(3): 309-345.

- Hawkes, P. J., Gouldby, B. P., Tawn, J. A. and Owen, M. W. 2002. "The joint probability of waves and water levels in coastal engineering design." *Journal of Hydraulic Research* 40(3): 241-251.
- Heffernan, J. E. and Tawn, J. A. 2004. "A conditional approach for multivariate extreme values (with discussion)." *Journal of the Royal Statistical Society: Series B (Statistical Methodology)* 66(3): 497-546.
- Huizinga, H.,J.2007. "Flood damage functions for UE member states, HKV Consultants, Implemented in the framework of the contract #382442-F1SC awarded by the European Commision -Joint Research Center"
- Jamieson, S., Lhomme, J., Wright, G. and Gouldby, B. 2012a. "Highly efficient 2D inundation modelling with enhanced diffusion-wave and sub-element topography." *Proc. Inst. Wat. Man.* 165(10): 581-595.
- Lhomme, J., Gutierrez-Andres, J., Weisgerber, A., Davison, M., Mulet-Marti, J., Cooper, A. and Gouldby, B. 2010. "Testing a new two-dimensional flood modelling system: analytical tests and application to a flood event." *Journal of Flood Risk Management* 3(1): 33-51.
- McMillan, H. K. and Brasington, J. 2007. "Reduced complexity strategies for modelling urban floodplain inundation." *Geomorphology* 90(34): 226-243.
- Mínguez, R., Espejo, A., Tomás, A., Méndez, F. J. and Losada, I. J. 2011. "Directional calibration of wave reanalysis databases using instrumental data." *J. Atmos. Oceanic Technol.* 28: pp 1466-1485.
- Penning-Rowsell, E. C., Johnson, C., Tunstall, S., Tapsell, S., Morris, J., Chatterton, J., Coker, A., Green, C. 2003. The Benefits of flood and coastal defence: techniques and data for 2003. Flood Hazard Research Centre, Middlesex University.
- Reguero, B. G., Menendez, M., Mendez, F. J., Minguez, R. and Losada, I. J. 2012. "A Global Ocean Wave (GOW) calibrated reanalysis from 1948 onwards." *Coastal Engineering* 65(0): 38-55.
- Serinaldi, F. 2011. "Analytical confidence intervals for index flow flow duration curves", *Water Resour. Res.*, 47, W02542, doi:10.1029/2010WR009408.
- Torres-Freyermuth, A.; Losada, I.J.; Lara, J.L., 2007. "Modeling of surf zone processes on a natural beach using Reynolds-Averaged Navier-Stokes equations", *Journal of Geophysical Research. Oceans*, 112, C09014. doi: 10.1029/2006JC004050
- USACE 1996. "Risk-based Analysis for Flood Damage Reduction studies". Engineer Manual EM 1110-2-1619